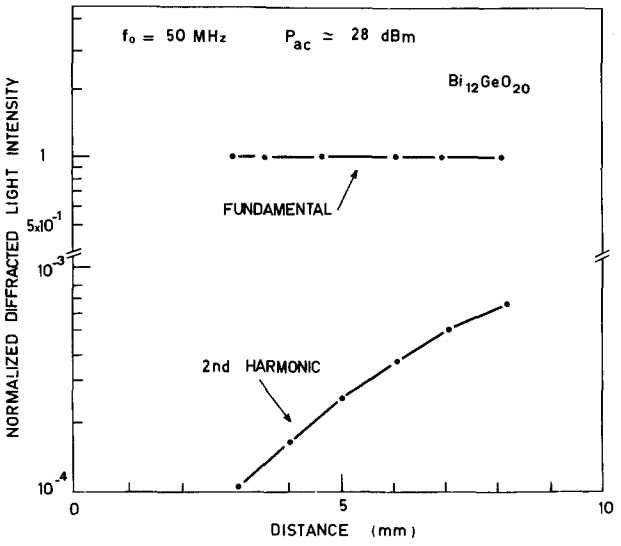

FIG. 2. Deflected light intensities as a function of interaction length illustrating second-harmonic generation investigated by transmission.

probing arrangements using a He-Ne laser.[6] The incident light is diffracted by the wave and detected by reflection or transmission at angles calculated for a line grating having a period equal to the acoustic wavelength. The diffracted angle measured $\theta_1 = 1°10'$ corresponds to a wave velocity of 1590 ± 5 m/sec, again in close agreement with the theoretical value. The attenuation of the wave along the crystal length was 0.1 dB/μsec.

At an angle $\theta_2 = 2\theta_1$, diffracted light was detected which corresponds to 100-MHz sound frequency indicating harmonic generation. The light intensity diffracted by the fundamental and the second-harmonic waves vs the interaction length is shown in Fig. 2. The second-harmonic power is proportional to the square of the interaction length and is obviously tied to acoustic nonlinear effects in the propagating medium. The very low level measured, 31.5 dB below the fundamental at a distance of 8 mm from the input transducer, does not influence the attenuation of the fundamental wave, in agreement with the independence of insertion loss with power previously obtained.

Moreover, the second-harmonic power is proportional to the square of the fundamental acoustic power used. Similar nonlinear effects have been reported in $LiNbO_3$ and in α quartz.[7-9]

In summary, we have computed the characteristics of Rayleigh waves propagating in the [001] direction on the $[1\bar{1}0]$ plane of $Bi_{12}GeO_{20}$. The results of our numerical analysis are in excellent agreement with direct measurements at 50 MHz of velocity using transducers and optical probing. With the latter technique we have detected second-harmonic generation due to nonlinear effects in the propagating medium up to a maximum acoustic power of 28 dBm.

Studies comparing the nonlinear effects in $Bi_{12}GeO_{20}$ with $LiNbO_3$ are currently being extended to higher frequencies.

We are grateful to E. L. Adler of McGill University for stimulating discussions.

[1]M. Onoe, A.W. Warner, and A.A. Ballman, IEEE Trans. Sonics Ultrasonics SU-14, 165 (1967).
[2]J.J. Campbell and W.R. Jones, J. Appl. Phys. 41, 2796 (1970).
[3]With new values for constants published by E.A. Kraut, B.R. Tittmann, L.J. Graham, and T.C. Lim [Appl. Phys. Letters 17, 271 (1970)], we obtained $(\Delta v/v)\times10^4 = 36$ and $k^2\times10^4 = 72$.
[4]W.R. Smith, H.M. Gerard, J.H. Collins, T.M. Reeder, and H.J. Shaw, IEEE Trans. Microwaves Theory and Techniques MTT-17, 865 (1969).
[5]J.J. Campbell and W.R. Jones, Trans. Sonics Ultrasonics SU-15, 209 (1968).
[6]A.J. Slobodnick, Jr., Appl. Phys. Letters 14, 94 (1969).
[7]A.J. Slobodnick Jr., J. Acoust. Soc. Am. 48, 203 (1970).
[8]E.G.H. Lean, C.C. Tseng, and C.G. Powel, Appl. Phys. Letters 16, 32 (1970).
[9]J. Kroskstad and L.O. Svaasand, Appl. Phys. Letters 11, 155 (1967).

APPLIED PHYSICS LETTERS VOLUME 19, NUMBER 12 15 DECEMBER 1971

Diffusivity and Solubility of Si in the Al Metallization of Integrated Circuits*

J.O. McCaldin and H. Sankur
California Institute of Technology, Pasadena, California 91109
(Received 19 July 1971; in final form 28 September 1971)

Si was diffused along the evaporated Al layer of an integrated-circuit structure at temperatures between 360 and 560 °C, and the resulting concentration profile analyzed by electron microprobe. The Si solubility was found to agree with literature values for Si in wrought Al. The Si diffusivity was found to be substantially enhanced, however, probably due to a high density of imperfections in the evaporated Al film. Our measured diffusivities indicate an activation energy $E_A \simeq 0.8$ eV, about 40% less than the value for Si in wrought Al.

The solid Al metallizations of integrated circuits are well known to dissolve silicon and to permit it to diffuse rapidly. This behavior is not surprising, however, as it is *qualitatively* just what earlier metallurgical studies[1,2] would lead one to expect. The present study of Si in the Al metallizations of inte-

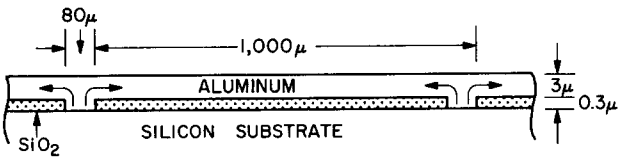

FIG. 1. Cross section of the prototype integrated circuit. Note that vertical dimensions are not to scale. Arrows suggest the predominantly horizontal diffusion path, typically 200 or 300 μ long.

grated circuits was undertaken to afford a *quantitative* comparison with the previous data. As will be described, Si was found to diffuse substantially more rapidly in the integrated-circuit situation than in wrought Al.

The prototype integrated circuit used in the present studies appears schematically in Fig. 1. Contact between Al and Si is prevented by the presence of SiO_2 everywhere except at the 80-μ-wide "cuts" in the oxide. The cuts serve as sources for Si diffusion, which proceeds along the 3-μ-thick Al layer for distances, typically, of 200—300 μ. Negligible loss of Si at the surface of the Al was assumed; otherwise the actual diffusivity would have been greater than is reported here and the observed concentration profiles would have been linear on the semilogarithmic plot of Fig. 2, instead of concave downward as was observed.

Preparation of the specimens was conventional, except that Al was evaporated onto the room-temperature substrate to a thickness some three times greater than is customary. The extra thickness of Al was needed in the subsequent microprobe analysis (to be described) to avoid excitation of the substrate Si. After preparation, a specimen, typically about $\frac{1}{4}\times\frac{1}{4}$ in. in area, was placed on a $\frac{1}{2}\times\frac{1}{2}$-in. preheated quartz platform and inserted into a hot quartz-lined tube furnace, through which dry argon flowed gently. A chromel-alumel thermocouple, calibrated at the melting point of Zn and sheathed in a $\frac{1}{8}$-in.-diam quartz tube, was placed next to the specimen. The specimen temperature was thus known to within an estimated ± 3 °C. The time required by the sheathed thermocouple (and thus, approximately, the specimen as well) to rise to within ~3 °C of its ultimate steady-state temperature was typically about 2 min. To minimize uncertainties in the time of effective heat treatment, the duration of heat treatment was never less than 20 min. After completion of the heat treatment, the specimen was removed from the furnace in about 2 sec and dropped onto a cool asbestos surface.

The Si that diffused from the oxide-cut "sources" into the metallization was detected by electron microprobe. A 10^{-4}-V 10^{-7}-A electron beam focused to ~5 μ in diameter was used, and counts at the SiK_α line were taken for 100 sec at a given location to determine the Si concentration [Si]. Starting at the edge of an oxide cut, [Si] was measured typically at 10- or 15-μ intervals until the signal was lost in background when [Si] $\lesssim 0.01\%$.

The [Si] measured over the oxide cuts[3] was taken to represent the solubility σ of Si in Al at the heat-treatment temperature, and the [Si] profile over the the remainder of the metallization was fitted by erfc to yield the diffusivity D. A typical example of a measured [Si] profile and the fitting of erfc to these data is shown in Fig. 2. The measured profiles were usually slightly more concave than could be fitted by an erfc; hence, two erfc fits were made, one fitting best in the high-concentration and the other best in the low-concentration regime. The diffusivity values corresponding to the two erfc fits typically differed by about 20%. However, larger discrepancies were occasionally found, the worst case of which is illustrated by the error bar shown in Fig. 4. As will be seen, however, even this uncertainty is small compared to the difference in D found for wrought and evaporated Al.

Another source of uncertainty in the experimental data should also be mentioned. A proper origin for the erfc fitting the data could only be estimated approximately. This is due primarily to the fact that the Si diffusion is not one dimensional when Si is "turning the corner" at the edge of the oxide cut. Also the edges of the oxide cuts did not always appear sharp after aluminization, so that an uncertainty in location of the origin of perhaps 10 μ was sometimes present. Some of the extra concavity in the experimental profiles may be due to this uncertainty.

A control specimen which had been processed through all steps except heat treatment exhibited zero [Si] in the microprobe.

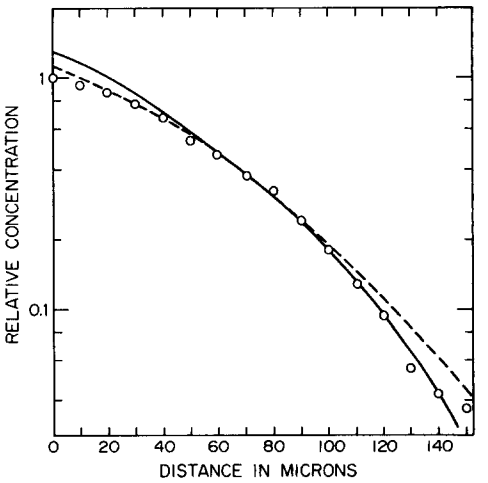

FIG. 2. A typical concentration profile of Si in evaporated Al as measured in the present experiments. In this example, specimen was heated 40 min at 446 °C. Two possible erfc fits to the experimental data are shown.

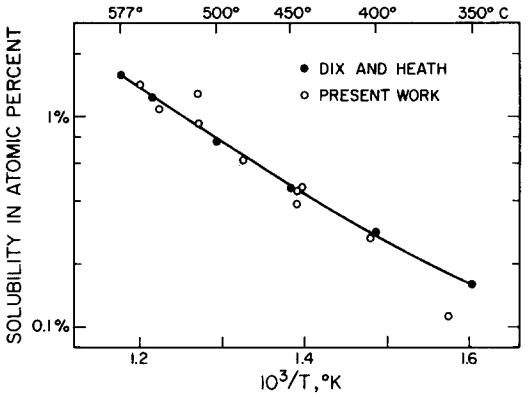

FIG. 3. Solubility of Si in solid Al according to previous investigators and the present investigators.

Figure 3 compares the solubility obtained in the present experiments with the metallographic data of Dix and Heath,[2] as reported by Hansen.[4] The latter states that these data are "generally considered to have the highest degree of accuracy"; it has been substantiated in a subsequent investigation by Glazov reported by Elliot.[5] Our microprobe measurements were subjected to the usual correction factors,[6] the principal factor being that due to absorption, with the over-all result $C_A = 1.44$, i.e., the measured intensities of the SiK_α line were increased by 44% to give [Si]. Although our measured solubilities show more scatter than those of Dix and Heath,[2] perhaps because of our difficulty[3] in identifying the maximum [Si], our measurements are in essential agreement with previous work.

Such is clearly not the case for our diffusivity measurements, however. As is readily apparent in Fig. 4, Si consistently diffuses more rapidly in the evaporated Al of an integrated circuit structure than in conventional Al specimens. When this result first became evident, we also prepared conventional Al specimens as follows: Al wire,[7] of 99.9999% purity and 0.6 mm in diameter, was pressed against a Si surface in dry argon and heated. Subsequently a 12° bevel section of the Si-Al bond was studied by electron microprobe. The [Si] profile was fitted by an erfc, yielding diffusivity values consistent with the metallurgical literature,[1,8-11] as indicated in Fig. 4.

Values for D from the metallurgical literature do scatter appreciably, as one sees in the figure. Because of this, an earlier writer[1] summarized the situation by giving a band of values for D, which is reproduced in Fig. 4. One explanation advanced for this variability in D is that D is concentration dependent. Matano-Boltzmann analysis[1,10] of diffusion profiles suggests that D decreases somewhat as [Si] increases. In any case, a best straight-line fit to the conventional D values of Fig. 4 would include all data points within a factor of 2.

On the other hand, when Si diffusivity is measured in integrated circuit specimens, D becomes enhanced as much as $1\frac{1}{2}$ orders of magnitude. Again, appreciable scatter is present, which in the present instance could arise from a variable degree of annealing of the imperfections one expects in evaporated Al. Specimens annealed at the same temperature but for different times do in fact show that the enhancement in D decreases somewhat for the longer annealing times, as shown in Fig. 4. However, this effect is small and we prefer to leave open the question of the origin of the large scatter in D. The over-all enhancement in D associated with integrated-circuit conditions is unmistakable, however, and we feel it is likely due to imperfections in the Al film. These imperfections occur initially during Al evaporation, which produces, at best, a very finely microcrystalline film. On heating, the amount of grain boundary in the film must decrease sharply, since later etching of the specimens indicates grains mostly with 3–10-μ diameters as viewed from above. However, other imperfections like dislocations could be expected to remain at high concentration, particularly as the differential thermal expansion of Si and Al would cause substantial working of Al in the diffusion path of the integrated circuit geometry, but much less so in conventional metallurgical specimens.

Whatever the origin of the observed enhancement in diffusivity, it is interesting to speculate on possible consequences for devices made in the Si-Al system. A recent LEED study[12] of Si evaporated onto Al crystals suggests that Si diffuses into bulk Al at temperatures slightly above ambient. If such is the case, an even more striking behavior could be expected in the Al of integrated circuits, provided one

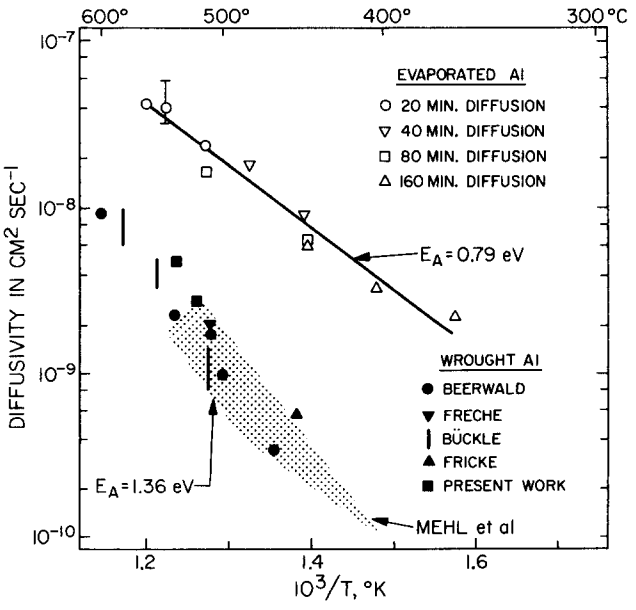

FIG. 4. The diffusivity of Si in solid Al. Conventional Al specimens, e.g., drawn wires and rolled sheets, are indicated by filled symbols. The evaporated Al of the present integrated-circuit specimens are indicated by open symbols.

is willing to extrapolate the present results to room temperature. At higher temperatures, such as are used to make Ohmic contacts and Schottky barriers in the Si-Al system,[13] the presently observed enhanced diffusivity suggests that consideration should be given to the ultimate disposition of the appreciable quantities of Si dissolved into the Al metallization. Also, in other choices of evaporated metal on semiconductor, these effects may occur at lower temperatures. For example, Hiraki *et al.*[14] have detected by their backscattering technique Si movement through an overlying Au film at 150 °C. Such transfer of Si through metal films could be quite useful in, for example, the formation of Ohmic contacts. This should be particularly true in the Si-Al or Ge-Al system, where Al incorporated in the semiconductor during growth would strongly dope it.

In conclusion, we find that Si diffuses more rapidly through the Al metallization of integrated circuits than through conventional wrought Al, and that the activation energy for diffusion in the former case is substantially reduced from the conventional value.

The authors wish to thank R. Cunningham, who operated the electron microprobe, and Dr. F.S. Buffington for advice on the physics of diffusion.

*Work supported in part by Eastman Kodak Research Grant in Solid State Science.

[1]R. F. Mehl, F. N. Rhines, and K. A. von den Steinen, Metals and Alloys 13, 41 (1941).
[2]E. H. Dix and A. C. Heath, Trans. AIME 78, 164 (1928).
[3]Actually the highest [Si] was measured *just outside* the oxide cuts and was taken to represent σ. This comes about because the Si substrate is a very effective nucleation center, and even our most rapidly cooled specimens lost some Si to the substrate over the oxide cuts, but not elsewhere, during quench.
[4]Max Hansen, *Constitution of Binary Alloys* (McGraw-Hill, New York, 1958), p. 133.
[5]Rodney P. Elliott, *Constitution of Binary Alloys, First Supplement* (McGraw-Hill, New York, 1965), pp. 55–56.
[6]T. O. McKinley, K. F. J. Heinrich, and D. B. Wittry, *The Electron Microprobe* (Wiley, New York, 1966), p. 125.
[7]Obtained from Cominco American, Spokane, Wash.
[8]H. R. Freche, Trans. AIME 122, 324 (1936).
[9]A. Beerwald, Z. Elektrochem. Angew. Phys. Chem. 45, 789 (1939).
[10]H. Bückle, Z. Elektrochem. 49, 238 (1943).
[11]William G. Fricke, Jr., ASM Trans. Quarterly 58, 421 (1965).
[12]F. Jona, J. Appl. Phys. 42, 2557 (1971).
[13]A. Y. C. Yu and C. A. Mead, Solid State Electron. 13, 97 (1970).
[14]A. Hiraki, M.-A. Nicolet, and J. W. Mayer, Appl. Phys. Letters 18, 178 (1971).

APPLIED PHYSICS LETTERS VOLUME 19, NUMBER 12 15 DECEMBER 1971

Efficient Parametric Mixing in CdSe†

R. L. Herbst and R. L. Byer
Microwave Laboratory, Stanford University, Stanford, California 94305
(Received 25 August 1971)

We have obtained the first phase-matched nonlinear interaction in CdSe and have observed a 35% conversion efficiency for mixing 10.6 μ with a pump at 1.833 μ to generate a signal at 2.2 μ. The mixing process phase matches at 77° to the optic axis and confirms the predicted phase-matching angle. The measured nonlinear coefficient value of 2.5×10^{-22} mks agrees with previous results. The mixing experiment shows than an angle-tuned or pump-tuned infrared parametric oscillator is possible using CdSe as the nonlinear element.

CdSe has been proposed as a potential nonlinear material in the infrared spectral region.[1] Its nonlinear coefficient has been previously measured[2] and recently remeasured.[3] However, the previous index-of-refraction and birefringence data[4,5] did not allow phase-matching curves to be predicted. We have remeasured the refractive index of CdSe and have verified that it phase matches over an extended region in the infrared.

CdSe has a wurtzite structure with 6 *mm* point-group symmetry. The components of nonlinear polarization are

$$\begin{aligned} P_x &= 2d_{15}E_zE_x, \\ P_y &= 2d_{15}E_zE_y, \\ P_z &= d_{31}E_x^2 + d_{31}E_y^2 + d_{33}E_z^2, \end{aligned} \tag{1}$$

where $d_{31}=d_{15}$ by Kleinman's symmetry. For a positive birefringent crystal only type-II phase matching is allowed with

$$\omega_3 = \omega_2 + \omega_1$$

and

$$n_3^0\omega_3 = n_2^e\omega_2 + n_1^0\omega_1. \tag{2}$$

Figure 1(a) shows the transmittance of as-grown CdSe and selenium-compensated CdSe. The material grows selenium deficient and must be compensated following growth to obtain semi-insulating crystals with resistivities of 10^8 Ω cm.[6,7] When properly compensated the transparency extends to 25 μ, where it is limited by two-phonon absorption. We compensated as-grown CdSe crystals by heating the crystals in a 2-atm selenium vapor for two weeks. Compen-